Supporting Information

In-situ sulfidation of porous sponge-like CuO/$SiW_{11}Co$ into Cu_2S/$SiW_{11}Co$ as stabilized and efficient counter electrode for quantum dot-sensitized solar cells

Qiu Zhang, Lu Jin, Yuekun Zhang, Tingting Zhang, Fengyan Li,* Lin Xu*

Key Laboratory of Polyoxometalate Science of Ministry of Education, Department of Chemistry, Northeast Normal University, Changchun, Jilin 130024, P. R. China

Corresponding authors Tel.: +86 431 85099765; Fax: +86 431 85099765.

E-mail addresses: lify525@nenu.edu.cn; linxu@nenu.edu.cn

1. Experimental section

1.1 Chemicals and materials

$Cu(NO_3)_2 \cdot 3H_2O$ (AR, ≥99.5%), $(NH_2)_2CO$ (AR, ≥99.0%), $H_4SiW_{12}O_{40} \cdot xH_2O$ (AR, ≥99.5%), $C_4H_6CuO_4 \cdot H_2O$ (AR, ≥98.0%), Terpineol ($C_{10}H_{18}O$, AR), NH_4Cl (AR, ≥99.0%), H_2NCSNH_2 (AR, ≥99.0%), $C_4H_6O_4Zn \cdot 2H_2O$ (AR, ≥99.0%), KCl (AR, ≥99.5%), Na_2SO_3 (AR, ≥97.0%), absolute methanol and acetone were purchased from Sinopharm. $Na_2S \cdot 9H_2O$ (AR, ≥98.0%), Sulfur (S, 99.99%), Titanium oxide (TiO_2, Degussa, P25). $CdCl_2$ (AR, ≥99.0%), $CdSO_4$, (AR, 99.0%), $N(CH_2COONa)_3$ (AR, 98.0%), selenium powder (Se, 200 mesh, 99.9%) were purchased from Shanghai Aladdin Biochemical Technology Co., Ltd.

1.2 Synthesis of $SiW_{11}Co$

$H_4SiW_{12}O_{40} \cdot xH_2O$ (SiW_{12}) (2 mmol) is dissolved in a certain amount of water, and heating to 85°C. Take an appropriate amount of cobalt acetate solution, adding it dropwise to the above solution and continually heating 20 min at 85°C. After cooling to room temperature, add acetone to the obtained precipitate, dissolving and filting the solution. Then continue to add acetone until no precipitation occurs. Finally, evaporate the acetone at 65°C and dry it at 50°C for 10h to obtain the product.

2. Characterizations

X-ray powder diffraction test was conducted from 15 to 80° adopting Siemens D5005 diffractometer with Cu target Kα (λ = 1.5418 Å) rays as X-ray source. A field emission scanning electron microscope (SEM JEOL JSM 4800F) equipped with X-ray energy dispersion (EDX) analysis was used to study the surface morphology and element composition of the samples. X-ray photoelectron spectroscopy (XPS) was carried out applying an ESCALABMKII spectrometer and the X-ray source was achromatic Al-Ka (1486.6 eV). The electron transmission microscopy (TEM) and HRTEM images was received using the transmission electron microscope JEOL-2100F. The datas of nitrogen adsorption–desorption isotherms were collected from an ASAP 2020 (Micromeritics, USA). An IVIUM purchased from Tianjin Brillante Technology Limited with a filtered 500 W Xenon lamp is utilized to current–voltage (I–V) curves measurements under the condition of AM 1.5 100 mW cm^{-2}. The EIS, Tafel, CV and open circuit voltage decay (OCVD) tests are all used CHI660D electrochemical workstation (Shanghai Chenhua, China). EIS test conditions: the frequency range is 10^{-1}-10^5 Hz; the amplitude is 0.01 V, which is performed under the condition of open-circuit voltage. All characterizations were conducted at ambient temperature and pressure.

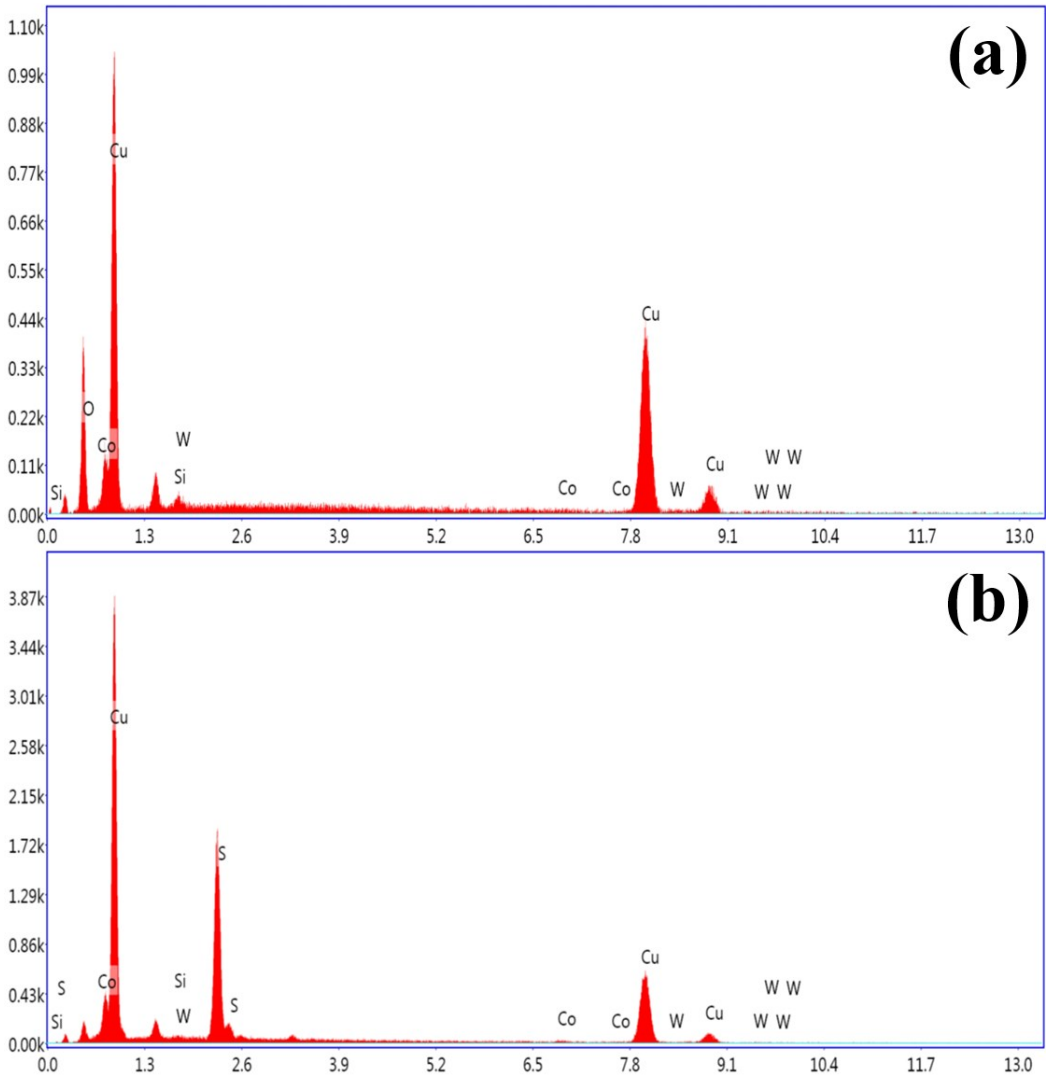

Fig. S1. EDX images of (a) CuO-2 and (b) Cu_2S-2

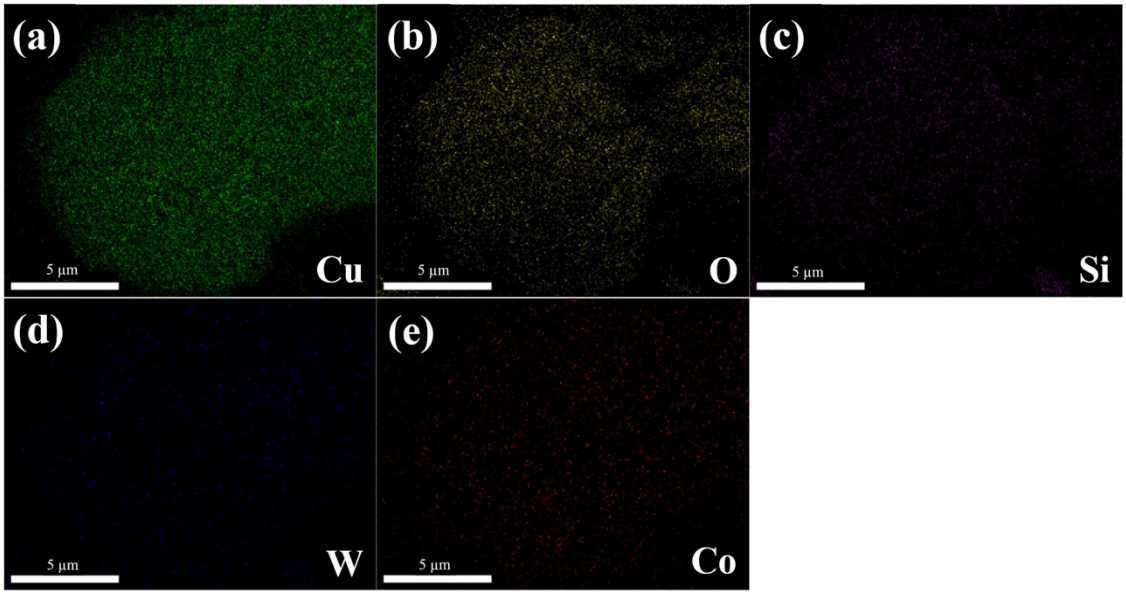

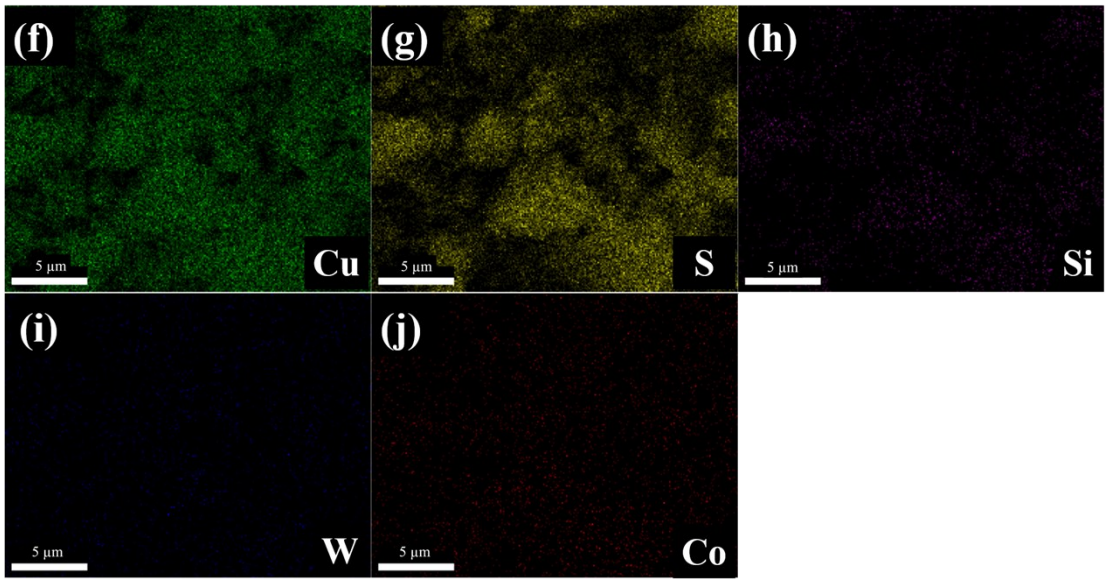

Fig. S2. (a-e) EDX elemental mappings of (a) Cu, (b) O, (c) Si, (d) W, (e) Co in as-prepared CuO-2 sample. (f-j) EDX elemental mappings of (f) Cu, (g) S, (h) Si, (i) W, (j) Co in Cu_2S-2 sample.

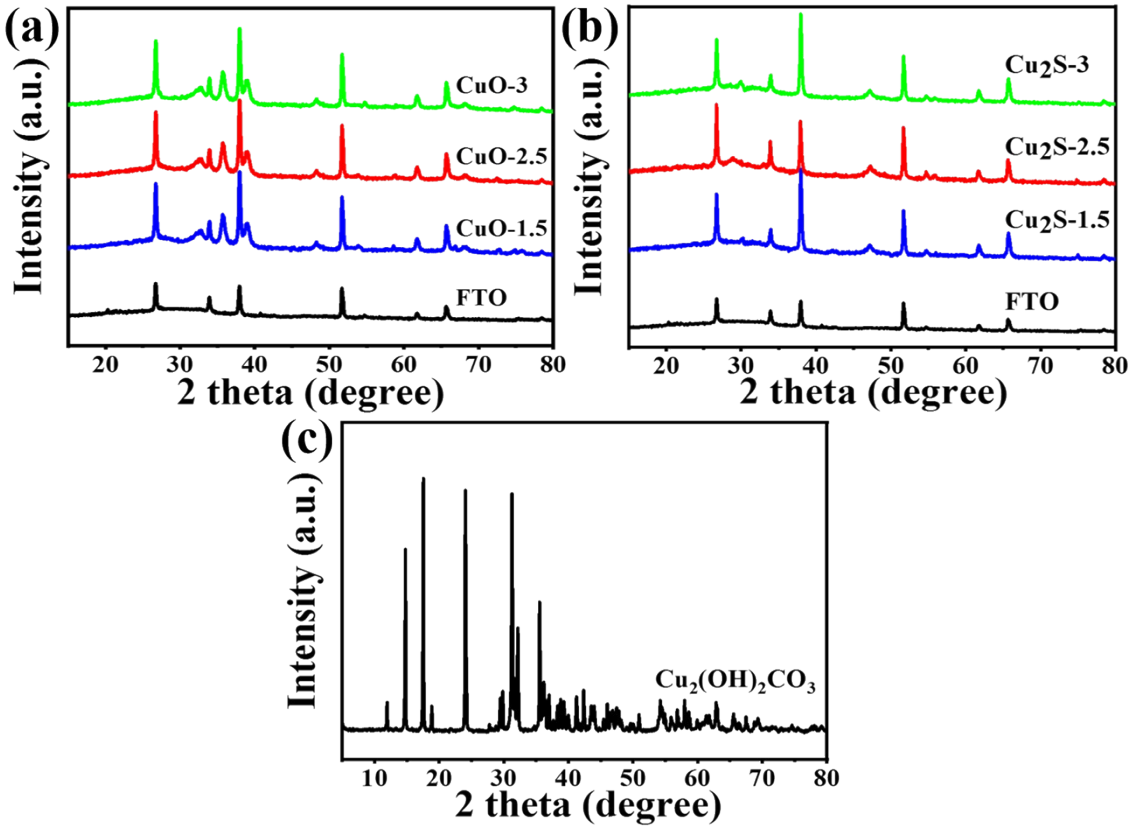

Fig. S3. XRD patterns of (a) CuO, (b) Cu_2S with different $SiW_{11}Co$ doping ratio. (c) XRD of $Cu_2(OH)_2CO_3$ precursor.

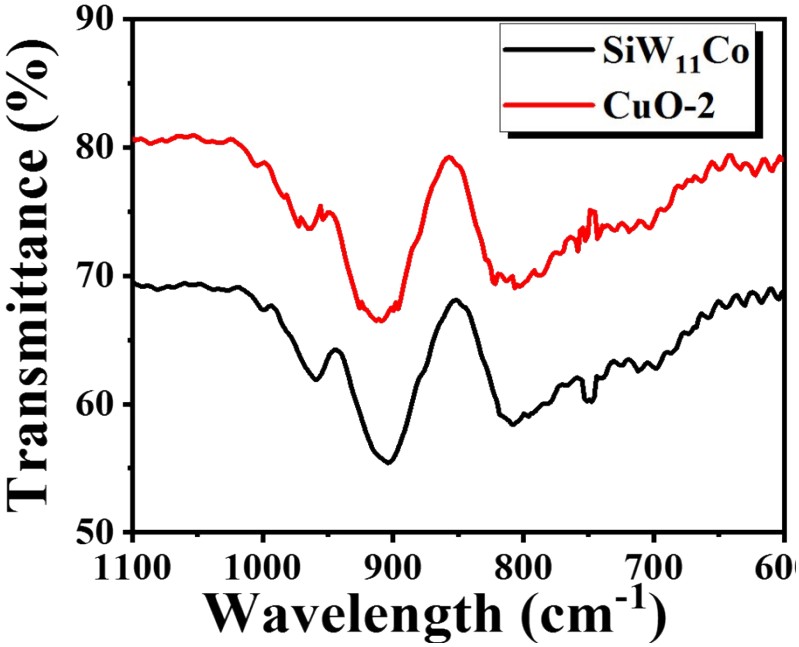

Fig. S4. IR spectrogram of SiW11Co and CuO-2 product.

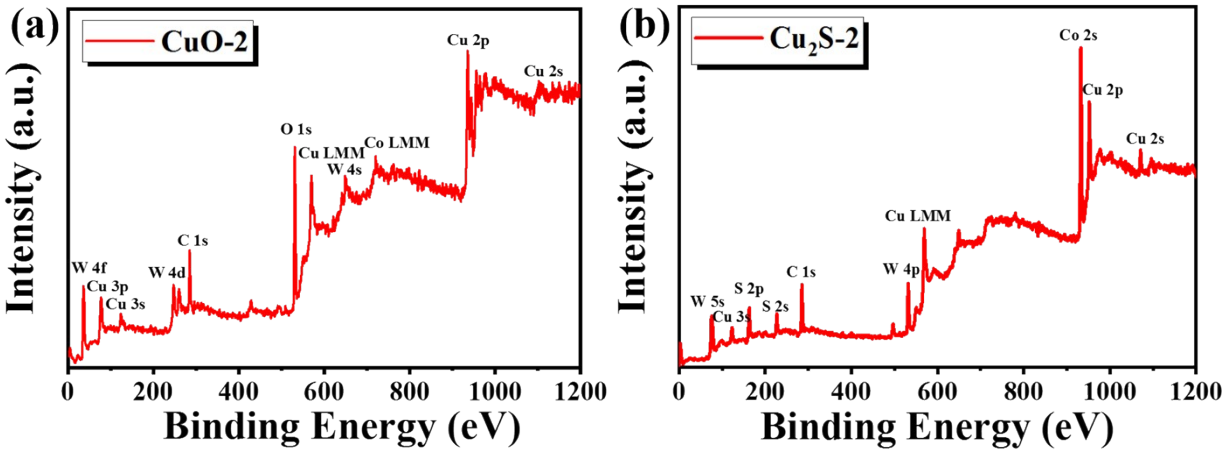

Fig. S5. XPS survey spectrum of (a) CuO-2 and (b) Cu_2S-2.

Table S1. Detailed BET datas for different samples.

Sample	S_{BET} (m^2/g)	Pore volume (cm^3/g)	Pore width (nm)
CuO	40.38	0.19	17.52
CuO-2	54.78	0.22	17.46

Table S2. Performances parameters of QDSSCs assembled with different CEs.

Counter electrode	J_{sc} (mA/cm^2)	V_{oc} (V)	FF	PCE (%)
Cu_2S-2.5	21.42	0.53	0.49	5.71
Cu_2S-1.5	21.50	0.52	0.48	5.42
Cu_2S-3	20.00	0.53	0.46	5.04

Table S3. Electrochemical parameters of different counter electrodes films.

Counter electrode	R_s (Ω)	R_{ct} (Ω)	J_0 (mA/cm^2)	τ_e (ms)
Cu_2S-2.5	2.210	0.276	2.22	43.91
Cu_2S-1.5	2.364	0.282	1.60	36.69
Cu_2S-3	2.489	0.293	1.59	32.60

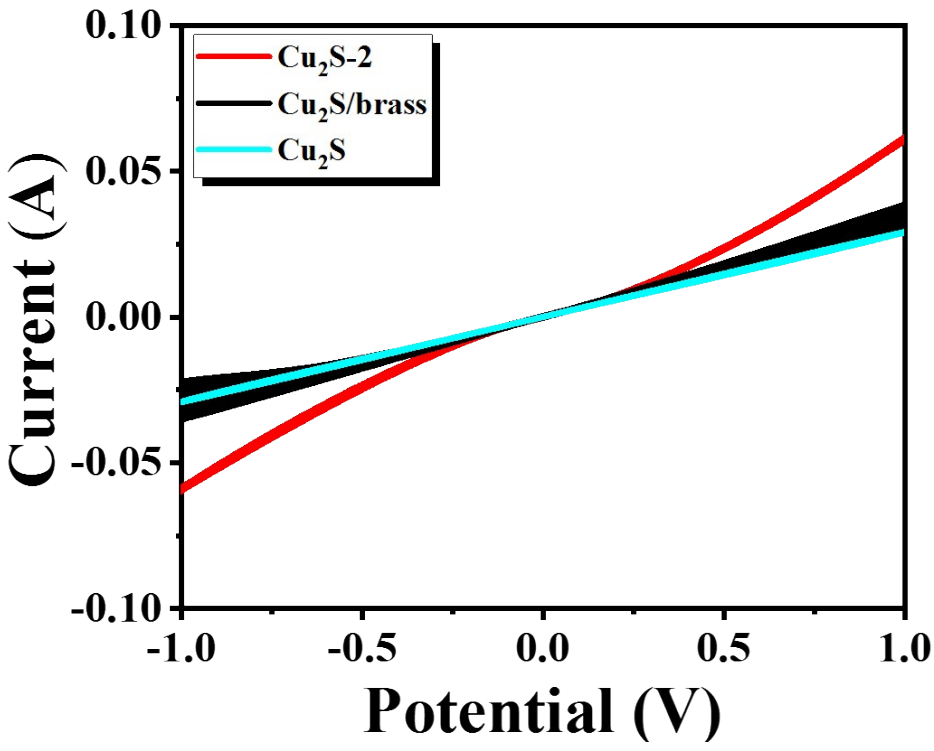

Fig. S6. 10 cycles of CV plots of the symmetrical dummy cells with various CEs in the dark.

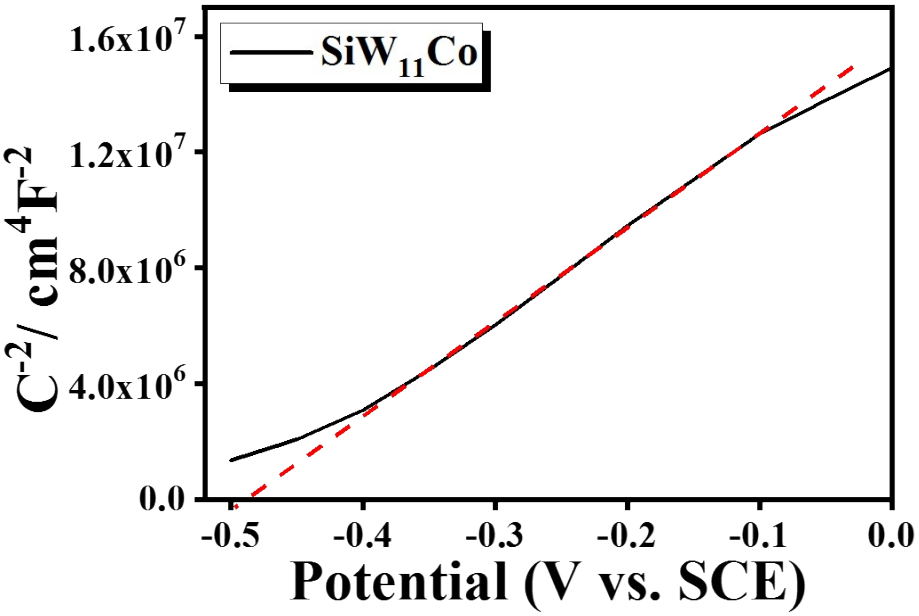

Fig. S7. Mott-Schottky curve of $SiW_{11}Co$.

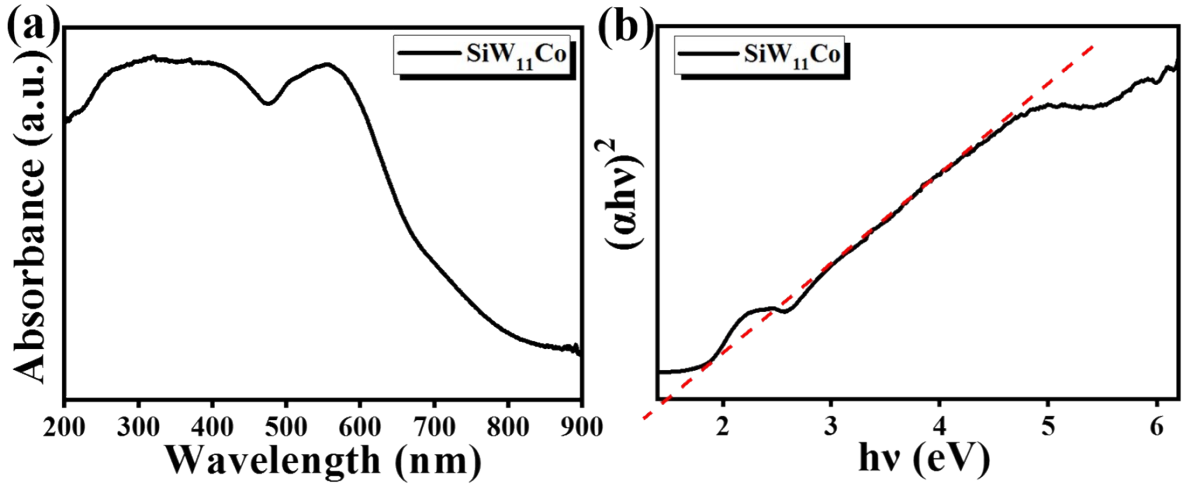

Fig. S8. UV-visible diffuse reflectance spectrum (a) and the band gap calculation (b) of $SiW_{11}Co$.

Method of obtaining $SiW_{11}Co$ CB or VB:

As can be obtained from Fig. S7, the value of $SiW_{11}Co$ E_{CB} is -0.491 V (vs. SCE). According to the formula of $E_{RHE} = E_{SCE} + 0.241$ (ref. Applied Catalysis A: General 2017, 536, 67.), E_{CB} = -0.25 V (vs. NHE, -4.25 V vs. AVS). Besides, from the band gap spectra in Fig. S8, we can calculate the E_g of $SiW_{11}Co$ is 1.51 eV, on the basis of $E_g = E_{CB} - E_{VB}$, the E_{VB} of $SiW_{11}Co$ is +1.26 V (vs. NHE, -5.76 V vs AVS).

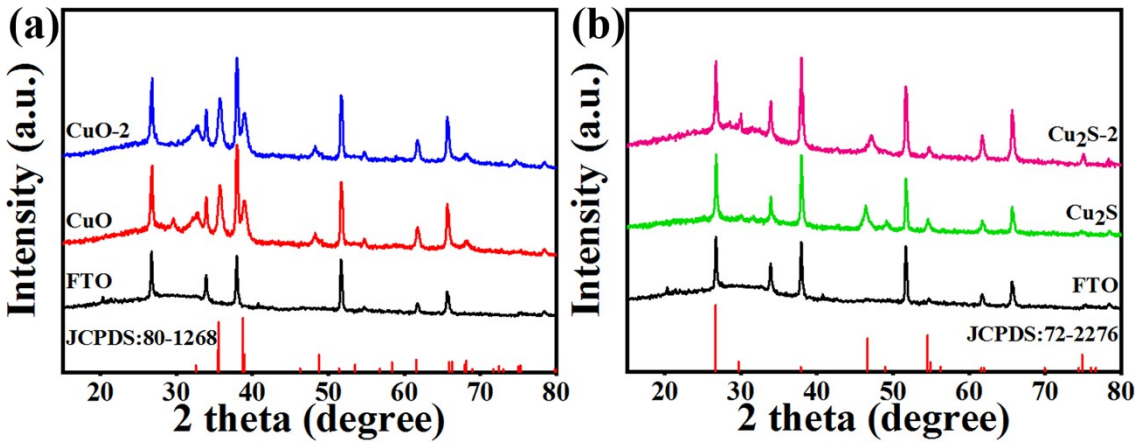

Fig. S9. XRD patterns of (a) CuO, CuO-2, (b) Cu_2S, Cu_2S-2 films on FTO.

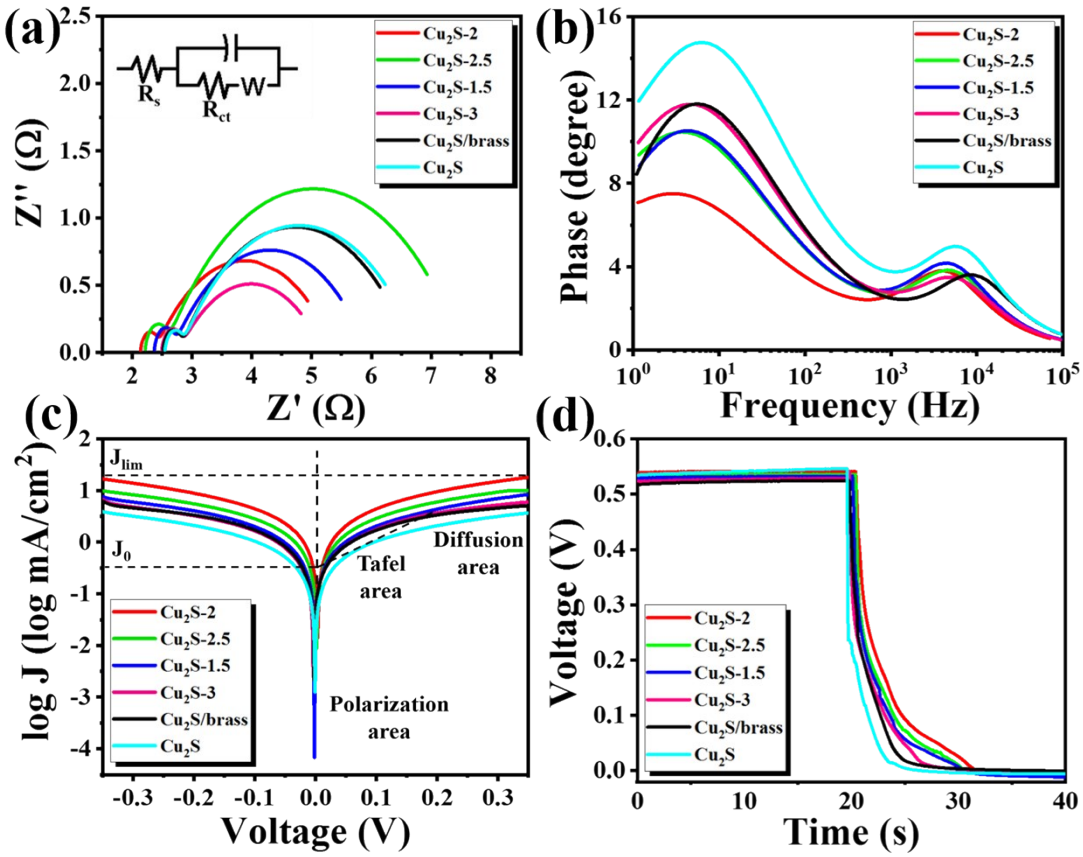

Fig. S10. (a) EIS Nyquist plots, the inset shows the equivalent circuit, (b) Bode phase curves and (c) Tafel polarization curves of the symmetric cells based on various CEs, (d) OCVD plots of differernt CEs films.

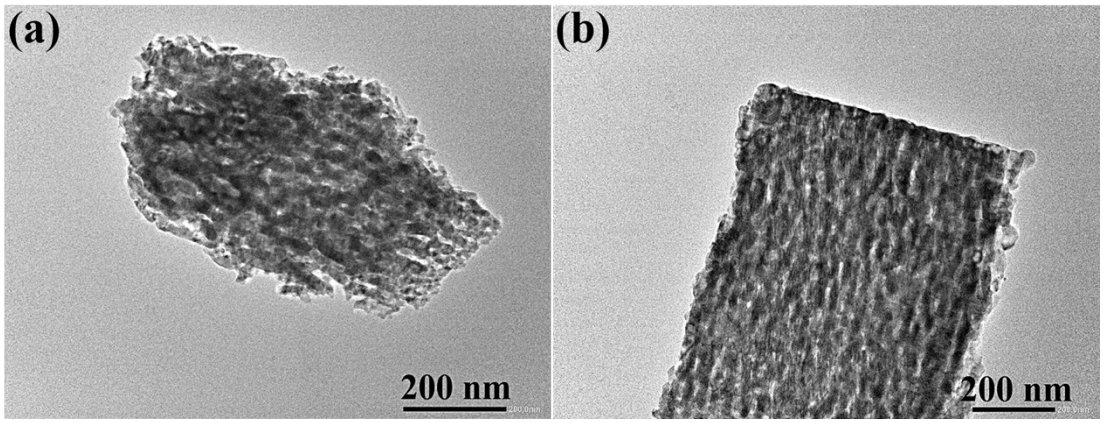

Fig. S11. TEM of CuO (a) and CuO-2 (b).

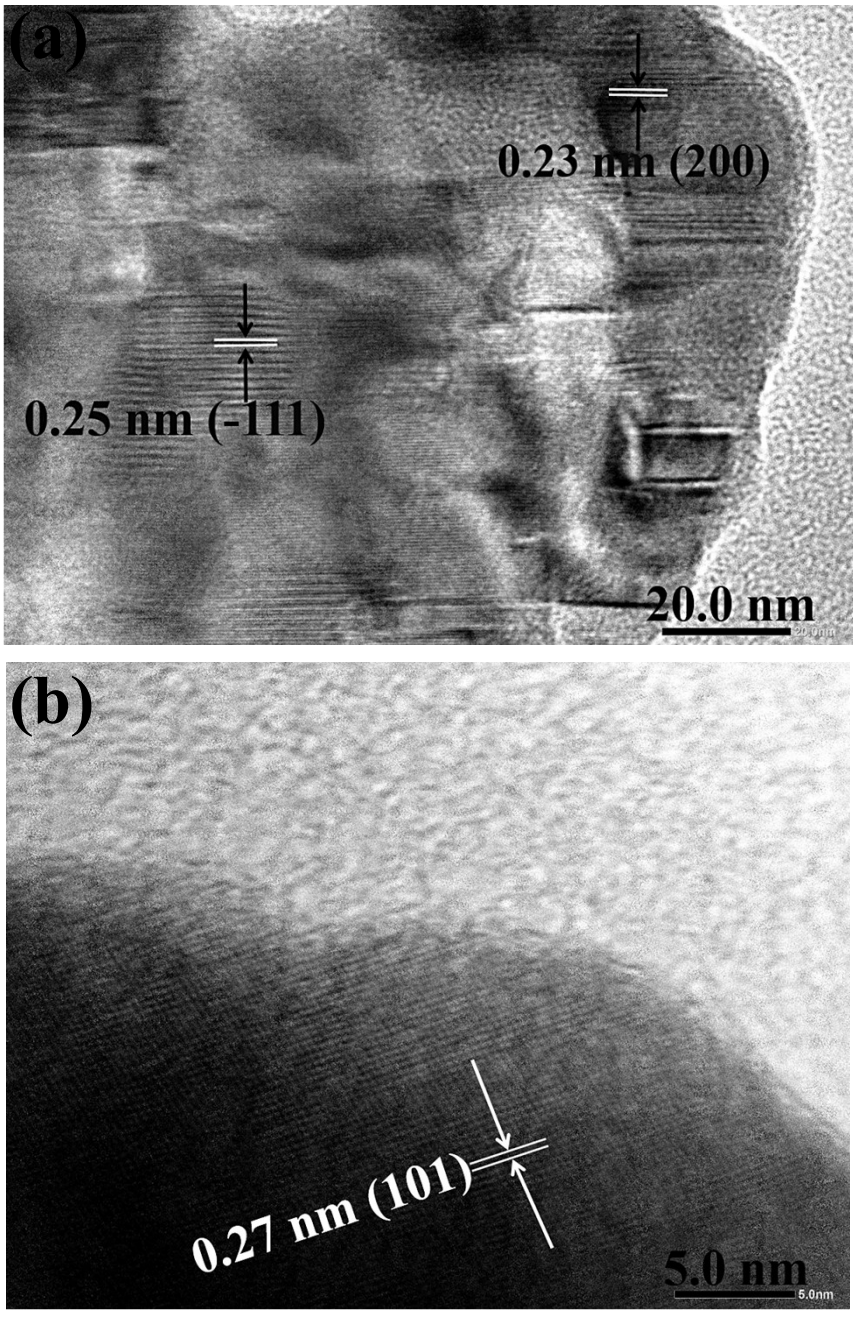

Fig. S12. HRTEM of CuO-2 (a) and Cu_2S-2 (b).

Table S4. Result comparisons of present performance parameters with other reports of similar counter electrodes.

Counter electrode	QD	R_s (Ω)	J_0 (mA/cm^2)	J_{sc} (mA/cm^2)	V_{oc} (V)	FF	PCE (%)	Reference
Cu_2S-2	CdS/CdSe	2.134	3.45	21.33	0.54	0.52	5.94	Present work
Cu_2S/brass	CdS/CdSe	2.511	1.52	16.42	0.57	0.53	4.96	Present work
Cu_2S	CdS/CdSe	2.542	1.36	20.33	0.53	0.45	4.93	Present work
Cu_2S	CdS/CdSe	2.93	/	15.71	0.48	0.42	3.16	[1]
RGO/Cu_2S-2	CdS/CdSe	2.48	/	17.11	0.58	0.48	4.76	[1]
Cu_2S	CdS/CdSe	/	/	11.69	0.60	0.44	3.18	[2]
Electrodeposited CuS	CdS/CdSe	2.50	0.54	16.05	0.55	0.48	4.32	[3]
Spray pyrolyzed Cu_2S	CdS/CdSe	/	/	14.30	0.51	0.51	3.75	[4]
CuS/brass	CdS/CdSe	2.97	0.006	17.40	0.38	0.58	3.82	[5]
Cu_2S(5)on ITO	CdSe	/	/	17.70	0.55	0.49	4.78	[6]
Cu_2S/carbon	CdS/CdSe	8.23	/	13.69	0.59	0.48	3.87	[7]
$Cu_{1.8}S$	CdS/CdSe	6.11	/	16.07	0.50	0.41	3.30	[8]
CuS	CdS/CdSe	6.53	/	15.08	0.51	0.51	3.95	[8]
Cu_2S	CdS/CdSe	12.14	/	13.45	0.45	0.60	3.65	[9]
Cu_2S	CdS/CdSe	26.12	/	13.05	0.51	0.63	4.22	[10]

Reference

[1] B. Yuan, Q. Gao, X. Zhang, L. Duan, L. Chen, Z. Mao, X. Li and W. Lü, *Electrochim. Acta*, 2018, **277**, 50-58.

[2] H. Salaramoli, E. Maleki, Z. Shariatinia and M. Ranjbar, *J. Photoch. Photobio. A*, 2013, **271**, 56-64.

[3] F. Wang, H. Dong, J. Pan, J. Li, Q. Li and D. Xu, *J. Phys. Chem. C*, 2014, **118**, 19589-19598.

[4] G. S. Selopal, I. Concina, R. Milan, M. M. Natile, G. Sberveglieri and A. Vomiero, *Nano Energy*, 2014, **6**, 200-210.

[5] W. Liang, L. Zhu, H. Liu, F. Xi and W. Li, *Electrochim. Acta*, 2015, **184**, 285-294.

[6] C. Shen, L. Sun, Z. Y. Koh and Q. Wang, *J. Mater. Chem. A*, 2014, **2**, 2807-2813.

[7] D. M. Li, L. Y. Cheng, Y. D. Zhang, Q. X. Zhang, X. M. Huang, Y. H. Luo, Q. B. Meng, *Sol. Energy Mat. Sol. C.*, 2014, **120**, 454-461.

[8] M. Ye, X. Wen, N. Zhang, W. Guo, X. Liu and C. Lin, *J. Mater. Chem. A*, 2015, **3**, 9595-9600.

[9] Y. Y. Yang, Q. X. Zhang, T. Z. Wang, L. F. Zhu, X. M. Huang, Y. D. Zhang, X. Hu, D. M. Li, Y. H. Luo and Q. B. Meng, *Electrochim. Acta*, 2013, **88**, 44-50.

[10] S. Wang, Q. X. Zhang, Y. Z. Xu, D. M. Li, Y. H. Luo and Q. B. Meng, *J. Power Sources*, 2013, **224**, 152-157.